Proceedings of the Korean Nuclear Society Autumn Meeting
Seoul, Korea, October 1999

A Pin Power Reconstruction Method for CANDU Reactor Cores

Hyung-Seok Lee*, Won Sik Yang and Man Gyun Na
Chosun University, Department of Nuclear Engineering
375 Seosuk-dong, Dong-gu, Kwangju 501-759, Korea

Hangbok Choi
Korea Atomic Energy Research Institute
P.O. Box 105, Yuseong, Taejon 305-600, Korea

Abstract

A reconstruction method has been developed for recovering pin powers from CANDU core calculations performed with the coarse-mesh finite-difference diffusion approximation and single-assembly lattice calculations. The homogeneous intra-nodal distributions of group fluxes are efficiently computed using polynomial shapes constrained to satisfy the nodal information approximated from the node-average fluxes. The group fluxes of individual fuel pins in a heterogeneous fuel bundle are determined using these homogeneous intra-nodal flux distributions and the form functions obtained from the single-assembly lattice calculations. The pin powers are obtained using these pin fluxes and the pin power cross sections generated by the single-assembly lattice calculation. The accuracy of the reconstruction schemes has been estimated by performing benchmark calculations for partial core representation of a natural uranium CANDU reactor. The results indicate that the reconstruction schemes are quite accurate, yielding maximum pin power errors less than ~3 %. The main contribution to the reconstruction error is made by the errors in the node-average fluxes obtained from the coarse-mesh finite-difference diffusion calculation; the errors due to the reconstruction schemes are less than 1 %.

I. Introduction

In the Canada deuterium uranium (CANDU) reactor, fuel elements experience changes of linear power during their residence in a fuel channel because of on-power refueling. The linear power change and the ramped power of the fuel element itself are essential to determining fuel integrity parameters such as the stress corrosion cracking failure probability. Thus it is necessary to estimate the detailed power distribution inside a fuel bundle accurately, especially for the advanced CANDU fuels under development, including the recycled uranium, the slightly enriched uranium, the mixed oxide, and the spent PWR fuel. These fuels are expected to have larger flux gradients than the natural uranium fuel because of a higher discharge burnup. In addition, the irradiation test of these advanced fuels in a research reactor also requires the intra-bundle power distribution to predict the irradiation behavior of each fuel element. However, it is difficult to obtain the detailed pin-wise information using the current analysis tool. This has motivated development of a method to predict the fuel element power distribution of a CANDU fuel bundle using information from two-dimensional lattice calculations and three-

* Korea Atomic Energy Research Institute

dimensional core calculations.

The methods used to recover detailed pin-wise information from coarse reactor representations, usually referred to as reconstruction methods, have reached a high level of development for light water reactors[1-7] and liquid metal reactors[8,9]. These reconstruction methods have become standard analysis tools because they extend the usefulness of computationally efficient nodal schemes and eliminate the need to perform full-core fine-mesh computations. All these methods intuitively assume that the detailed flux shape in an assembly can be approximated by superposing detailed inner assembly form functions on a smoother intra-nodal shape function. The assembly form function is derived from the single assembly calculations, and the intra-nodal flux shapes are derived from the nodal solution consisting of nodal fluxes and surface currents. In general, the methods developed for the reconstruction of homogeneous intra-nodal fluxes include polynomial[2,3,8] and exponential interpolation methods[4,5], analytical methods[6], and direct solver methods based on finite-difference techniques[7,9].

However, because the current design and analysis tool for CANDU reactors, RFSP[10], is based on a coarse-mesh finite-difference scheme, existing reconstruction methods developed for nodal methods are not directly applicable to CANDU reactor analysis. Here we describe techniques for reconstructing pin-wise power distributions of a CANDU fuel bundle based on full-core diffusion calculations performed on a coarse-mesh finite-difference scheme of the RFSP code system. The details of the reconstruction methods are described in Sect. 2 and the results of numerical tests are presented in Sect. 3. Finally, Section 4 concludes the paper.

II. Reconstruction Methods

Since the CANDU reactor is a thermal reactor, it is natural to use the lessons learned from the reconstruction methods developed for light water reactors (LWRs). The reconstruction methods for LWRs can be divided into two categories; the form function method[2,4,5] and the embedded calculation method[11]. In the CANDU fuel bundle, however, fuel elements are arranged in a cluster form as shown in Fig. 1, rather than a regular square or triangular array, which makes it difficult to determine the pin powers using the embedded calculation method. Therefore, it was decided to adopt the form function method in this study.

In order to test the applicability of the form function method to reconstruct the pin power of CANDU fuel bundles, a preliminary study was performed using the HELIOS[12] lattice analysis code. In the preliminary study, a multi-assembly problem was constructed, which is composed of fresh and burned fuel bundles. The two-group fluxes were calculated with HELIOS and compared to those of single assembly calculations. It was found that the ratios of the multi-assembly fluxes to the corresponding single-assembly fluxes are smooth functions of position. This result suggests that, for each energy group g, the detailed flux shape in a fuel bundle can be approximated by synthesizing the single-assembly flux shape and the smoother intra-nodal shape function such as:

$$\phi_g(x,y) = \hat{\phi}_g(x,y) \times H_g(x,y) . \tag{1}$$

The single-assembly flux shape, H_g, is referred to as the form function, and can be obtained as a function of burnup in the course of generating group constants. Therefore, if the intra-nodal shape function $\hat{\phi}_g$ can be obtained accurately from the core calculation performed with homogenized group constants, the detailed flux

shape in a fuel bundle can be determined using Eq. (1).

In the nodal methods for LWR analysis, the homogeneous intra-nodal flux shape is generally obtained by expanding it with predetermined functions and determining the expansion coefficients using the nodal solution consisting of node-average fluxes and surface-average fluxes and currents. However, the RFSP code gives only node-average fluxes because it uses a coarse-mesh finite-difference scheme. Therefore, the intra-nodal flux shape for a node should be approximated using the node-average fluxes of neighboring nodes. In this study, in order to simplify the derivation of the intra-nodal flux shape, we approximately determine the surface-average fluxes and currents and the corner point fluxes using the node-average fluxes of neighboring nodes.

II.A. Approximation of Surface-average and Corner Point Values

In order to determine the surface-average fluxes and currents, the planar flux distribution is assumed to be linear in each of the two nodes adjacent to a surface. By requiring the node-average fluxes to be reproduced and by enforcing additional continuity conditions on the surface-average flux and net current, the surface-average flux and current at the interface of nodes i and $i+1$ can be obtained respectively as:

$$f_s(h_i/2) = \frac{(D_i/h_i)\bar{f}_i + (D_{i+1}/h_{i+1})\bar{f}_{i+1}}{D_i/h_i + D_{i+1}/h_{i+1}} \tag{2}$$

and

$$J_s(h_i/2) = \frac{\bar{f}_i - \bar{f}_{i+1}}{h_i/2D_i + h_{i+1}/2D_{i+1}}, \tag{3}$$

where we delete the group index g for simplicity, and $\bar{f}_i$, D_i, and h_i represent the node-average flux, diffusion coefficient, and mesh size (in the direction perpendicular to the interface) of node i, respectively. For surfaces at the external boundary, similar expressions can be obtained using the boundary conditions.

The corner point fluxes are also approximated by assuming that the flux distribution is linear in each of four nodes surrounding a corner point. The expansion coefficients are determined by requiring the node-average fluxes to be reproduced, by enforcing additional flux continuity conditions at the interfaces and the corner point, and by imposing a source-free condition at the corner point. Consequently, an expression for a corner flux can be obtained as:

$$f_c = \frac{\sum_{i=1}^{4} \frac{D_i \bar{f}_i}{A_i A_{i+1}}}{\sum_{i=1}^{4} \frac{D_i}{A_i A_{i+1}}}, \tag{4}$$

where the node index i is cyclic and A_i denotes the area of interface between node $i-1$ and i. For corner points at the external boundary, similar expressions can be obtained using the boundary conditions.

II.B. Reconstruction of Intra-nodal Flux Distribution

Using the above surface-average fluxes and currents and corner point fluxes as well as the node-average flux, the intra-nodal group flux is approximated for every node by assuming the flux within a node is separable in the x-y plane and axial directions. With this separability assumption, the axial flux distribution is interpolated by a

quadratic polynomial. The expansion coefficients are determined by requiring the node-average flux and the top and bottom surface-average fluxes to be reproduced. For the x-y plane flux distribution, two combinations of the above nodal values are employed to investigate the effects of errors introduced in the approximation of surface-average quantities and corner point fluxes. In the first case (method I), the surface-average fluxes, the corner point fluxes, and the node-average flux are selected to be reproduced. In the second case (method II), the surface-average currents are additionally required to be reproduced.

If the x-y plane flux distribution $\hat{f}_g(x,y)$ is interpolated for each group g by a polynomial in an N-dimensional polynomial space F_N, then it can be represented as:

$$\hat{f}_g(x,y) = \sum_{n=1}^{N} c_n^g f_n(x,y), \tag{5}$$

where $\{f_1, f_2, \Lambda, f_N\}$ is the basis of F_N. The expansion coefficients, c_n^g, are determined by requiring a selected set of nodal quantities to be reproduced. For selected nodal quantities to be reproduced in F_N, the linear functionals associated with these nodal quantities should be independent in the algebraic conjugate space of F_N [13]. Therefore, it is necessary to determine the minimum degree of the polynomial and the associated sets of basis functions with which the given nodal information can be reproduced.

For both of the above two cases, a fourth degree polynomial is required to reproduce the selected nodal quantities. The dimension of the fourth degree polynomial is 15, and hence greater than the number of constraints (9 for the method I and 13 for the method II). As a result, the interpolation polynomial cannot be determined uniquely with the given constraints. In order to determine the unique interpolation polynomial for selected nodal quantities, the subspaces of dimension equal to the number of constraints were determined so that the associated linear functionals are independent in their conjugate spaces. Among these subspaces, in consideration of symmetry, the biquadratic polynomial space was selected for the first case. For the second case, the subspace composed of all the monomials of the fourth order polynomial space except for xy^3 and x^3y was selected.

The linear functional associated with each nodal quantity can be evaluated analytically in polynomial spaces[8]. As a result, the coefficients of basis monomials in Eq. (5) are obtained as linear combinations of selected nodal quantities, and the interpolation polynomial is uniquely determined. That is, for a given set of node-average flux $\bar{f}_g$, surface-average fluxes f_{gi}^s, corner point fluxes f_{gi}^c, and surface-average net currents J_{gi}^s, the x-y plane distribution of the g-th group flux is determined as:

$$\hat{f}_g(x,y) = \bar{f}_g F^{av}(x,y) + \sum_{i=1}^{4} \left\{ f_{gi}^s F_i^s(x,y) + f_{gi}^c F_i^c(x,y) + J_{gi}^s F_i^J(x,y) \right\}, \tag{6}$$

where F's are the cardinal functions[14] corresponding to individual nodal quantities. The last term in Eq. (6) is obviously omitted in the first case, where the surface-average currents are not used.

The functional forms of cardinal functions depend on the selected nodal quantities and basis monomials. The cardinal functions of the above two reconstruction methods are shown in Tables 1 and 2 for the coordinate system shown in Fig. 2. The cardinal functions of each reconstruction method form a biorthonormal set for the

linear functionals corresponding to the selected nodal quantities. For example, the cardinal function F^{av} of the second case yields a unity value when averaged over the node, but zero value when averaged over a surface, when evaluated at a corner, or when its normal derivative is taken and averaged over a surface.

III. Numerical Tests

The accuracy of the above reconstruction methods has been tested by performing benchmark calculations for partial core representations of a natural uranium CANDU reactor. For more realistic evaluation, it was decided to generate the reference solutions with detailed collision probability calculations using the HELIOS code. Because of the limitation of the HELIOS code to two-dimensional calculations and the excessive computational time, however, two-dimensional calculations were performed for 3-by-3 and 6-by-6 fuel bundle problems. The burnup distribution of the 6-by-6 fuel-bundle problem was taken from a natural uranium CANDU core, but that of the 3-by-3 fuel-bundle problem model was arbitrarily assigned.

The reference solutions were obtained from HELIOS calculations by retaining the detailed internal structure of individual fuel bundles. The 89-group library was used in these calculations, and the reflective boundary condition was employed as the external boundary conditions. The form functions and homogenized group constants were generated as a function of burnup from the HELIOS calculation for a unit cell composed of a fuel bundle and surrounding moderator. The power cross sections of individual fuel pins were also edited to calculate the pin powers from the reconstructed pin fluxes. Using these group constants, two-group diffusion calculations were performed by representing each assembly by a single mesh. These calculations were performed using the finite-difference option of the DIF3D code[15], since the RFSP code is not flexible enough to solve these small problems.

III.A. Reconstruction Error

Using the node-average fluxes obtained from the coarse-mesh finite-difference diffusion calculation, the homogeneous intra-nodal flux distributions were reconstructed as described in the previous section. By evaluating these homogeneous intra-nodal flux distributions at individual fuel positions and multiplying the resulting fluxes by the corresponding form function values, the group fluxes in each fuel element were determined. The pin powers were obtained using these pin fluxes and the pin power cross sections generated in the single-assembly HELIOS calculation. The reconstructed group fluxes and power of each fuel element were compared to the reference solution.

Figure 4 shows for individual fuel bundles the maximum errors in the pin-wise group fluxes and powers reconstructed with reconstruction method I. The maximum errors in the reconstructed fast and thermal fluxes of the 3-by-3 fuel-bundle problem are 3.17 and 2.36 %, respectively. In the case of the 6-by-6 problem, they are 4.53 and 3.47 %, respectively. The relative error of the fast flux is greater than that of the thermal flux, but the absolute error is greater in the thermal flux, since the thermal flux is about two times larger than the fast flux in CANDU reactors. The maximum error in the reconstructed pin power is 2.11 % for the 3-by-3 problem, and 3.18 % for the 6-by-6 problem. The pin powers are generally overestimated in relatively more reactive fuel bundles and underestimated in less reactive fuel bundles.

Compared to reconstruction method I, method II showed slightly larger reconstruction errors, even though

additional information (surface-average currents) was used. For example, the maximum errors in the reconstructed fast and thermal fluxes of the 3-by-3 fuel-bundle problem were 3.33 and 2.44 %, respectively. The maximum error in the reconstructed pin power was 2.18 %. This is due to the relatively large errors in the surface-average currents caused by the finite-difference approximation of flux derivatives.

III.B. Individual Error Sources

The reconstruction errors shown in Fig. 3 include the errors caused by the coarse-mesh finite-difference diffusion calculation as well as the approximations in the reconstruction procedure. In order to quantify the individual sources of error, separate interpolation calculations were also performed using the node-average fluxes selected from the reference solution. Using the node-average fluxes obtained from reference HELIOS calculations, the group fluxes and powers of individual fuel pins were reconstructed as described above. These calculations give the interpolation errors due to the reconstruction scheme itself.

Figure 5 shows the maximum interpolation errors in the pin-wise group fluxes and powers obtained with reconstruction method I. The maximum errors in the fast and thermal fluxes of the 3-by-3 problem are 0.70 and 0.68 %, respectively. In the case of the 6-by-6 problem, they are respectively 0.74 and 0.28 %. The maximum error in the reconstructed pin power is 0.61 % for the 3-by-3 problem, and 0.28 % for the 6-by-6 problem. Compared to the 3-by-3 problem, the 6-by-6 problem shows relatively smaller interpolation errors, which is due to the smoother flux distributions resulting from the relatively smoother burnup distribution. Reconstruction method II showed slightly larger interpolation errors as in the case of the reconstruction errors. For example, the maximum pin power error of the 3-by-3 problem was 0.80 %. This result showed that method II is inferior to method I due to the relatively large errors in the surface-average currents.

Comparing the reconstruction and the interpolation errors, it can be found that the errors in the node-average fluxes caused by the approximate diffusion calculation make a much larger contribution to the reconstruction error than the errors due to the reconstruction scheme itself. These results indicate that the reconstruction methods are quite accurate, yielding maximum errors in power and group fluxes of less than 1 %. For the 3-by-3 problem, the maximum errors in the node-average fast and thermal fluxes obtained from the coarse-mesh finite-difference diffusion calculation were 3.00 and 2.17 %, respectively. In the case of the 6-by-6 problem, they were as large as 3.58 and 3.25 %, respectively. The corresponding maximum errors in node-average powers were 2.03 and 3.07 % for the 3-by-3 and 6-by-6 problems, respectively. Therefore, if the accuracy of node-average fluxes is improved, the overall reconstruction error would be reduced significantly.

The node-average fluxes obtained from the coarse-mesh finite-difference diffusion calculation contain the errors caused by the two-group diffusion approximation, coarse-mesh finite-difference method, and group constant generation. By introducing these approximations separately, the individual sources of error were estimated. First of all, the error contribution attributable to the coarse-mesh finite-difference method was estimated by refining the mesh size. As shown in Fig. 5 for the multiplication factor, the finite-difference solution converges as the mesh size decreases. When the node-average fluxes collapsed from the converged finite-difference solution were used, the maximum error in the reconstructed pin powers of the 3-by-3 problem was reduced to 1.35 % from 2.11 %, but the error was still two times larger than the interpolation error. The error in node-average powers obtained from the converged finite-difference solution was as large as 1.34 %. In the case of the 6-by-6 problem, the maximum error in reconstructed pin powers was reduced to 2.69 % from

3.18 %, which is about ten times larger than the interpolation error. The error in node-average powers obtained from the converged finite-difference solution was still as large as 2.50 %.

The group constants generated from a single-assembly calculation contain the errors caused by the reflective boundary condition used in the collision probability calculation. The error attributable to the group constants generated from a single-assembly HELIOS calculation was estimated by repeating the two-group diffusion calculations using the group constants collapsed from the reference solutions. As shown in Fig. 5, the converged finite-difference solution obtained using the reference group constants reduces the error in the multiplication factor of the 3-by-3 problem by only ~0.05 %. The error in the node-average power was reduced by a maximum of ~0.3 % and by an average of ~0.1 %. These results indicate that the effects of group constant errors are relatively small compared with the errors due to the two-group diffusion approximation.

Consequently, it appears that the largest contribution to the errors in the node-average fluxes are made by the two-group diffusion approximation, followed by the coarse-mesh effect; the errors due to the group constants generated by a single-assembly HELIOS calculation are relatively small. The errors caused by the two-group diffusion calculation represent the combined effects of approximations in the homogenization, the group collapsing, and the diffusion theory. Further investigation is required for isolating individual effects, and this is left for future study.

IV. Conclusions

Techniques have been developed for the reconstruction of CANDU pin powers from core calculations performed with the coarse-mesh finite-difference diffusion approximation and single-assembly lattice calculations. The homogeneous intra-nodal distributions of group fluxes are efficiently computed using polynomial shapes constrained to satisfy the node-average values and the surface-average and corner point values approximated from the node-average fluxes of neighboring nodes. The group fluxes of individual fuel pins in a heterogeneous fuel bundle are determined by evaluating the homogeneous intra-nodal flux distributions at individual fuel positions and multiplying the resulting fluxes by the corresponding form function values. Then, the pin powers are obtained using the pin fluxes and the pin power cross sections generated in the single-assembly lattice calculation.

In order to test the accuracy of the reconstruction schemes, benchmark calculations have been performed for partial core representations of a natural uranium CANDU reactor. The test results indicate that the reconstruction schemes are quite accurate, yielding maximum pin power errors less than ~3 %. The main contribution to the reconstruction error is made by the errors in the node-average fluxes obtained from the coarse-mesh finite-difference diffusion calculation; the errors due to the reconstruction schemes are less than 1 %.

The largest contribution to the errors in the node-average fluxes appears to be made by the two-group diffusion approximation, followed by the coarse-mesh effect and the errors due to the group constants generated by a single-assembly lattice calculation are relatively small. The errors caused by the two-group diffusion calculation represent combined effects of approximations in the homogenization, the group collapsing, and the diffusion theory. Work is under way to isolate these effects and to devise a method to improve the accuracy of the node-average fluxes.

ACKNOWLEDGEMENT

This work was supported by the Korea Atomic Energy Research Institute (KAERI), under contract 98C-028.

REFERENCES

1. M. ABOUDY, A. GALPERIN, and M. SEGEV, "A Test of Main Stream Pin Power Reconstruction Methods," *Nucl. Sci. Eng.*, **122**, 395 (1996).
2. K. KOEBKE and M. R. WAGNER, "The Determination of the Pin Power Distribution in a Reactor Core on the Basis of Nodal Coarse Mesh Calculations," *Atomkernenergie*, **30**, 136 (1977).
3. H. S. KHALIL, P. J. FINCK, and A. F. HENRY, "Reconstruction of Fuel Pin Powers from Nodal Results," *Proc. Topl. Mtg. Advances in Reactor Computations*, Salt Lake City, Utah, March 28-31, Vol. I, p. 367, American Nuclear Society (1983).
4. K. KOEBKE and L. HETZELT, "On the Reconstruction of Local Homogeneous Neutron Flux and Current Distributions of Light Water Reactors from Nodal Schemes," *Nucl. Sci. Eng.*, **91**, 123 (1985).
5. K. R. REMPE, K. S. SMITH, and A. F. HENRY, "SIMULATE-3 Pin Power Reconstruction: Methodology and Benchmarking," *Proc. Int. Reactor Physics Conf.*, Jackson Hole, Wyoming, September 18-22, Vol. III, p. 19, American Nuclear Society (1988).
6. R. BÖER and H. FINNEMANN, "Fast Analytical Flux Reconstruction Method for Nodal Space-Time Nuclear Reactor Analysis," *Ann. Nucl. Energy*, **19**, 617 (1992).
7. H. FINNEMANN, R. BÖER, and R. MÜLLER, "Combination of Finite Difference and Finite Volume Techniques in Global Reactor Analysis," *Kerntechnik*, **57**, 216 (1992).
8. W. S. YANG, P. J. FINCK, and H. KHALIL, "Reconstruction of Pin Power and Burnup Characteristics from Nodal Calculations in Hexagonal Geometry," *Nucl. Sci. Eng.*, **111**, 21 (1992).
9. M. YAMAOKA, M. KAWASHIMA, T. YAMAGUCHI, and H. TAKASHITA, "A Method for Evaluation of Fuel Pin-wise Power Distribution in Fast Reactors," *Proc. Intl. Conf. on the Physics of Reactors*, Mito, Japan, September 16-20, Vol. 1, p. A-278, Japan Atomic Energy Research Institute (1996).
10. B. ROUBEN, "RFSP Program Description," TTR-370, Rev. 1, Atomic Energy of Canada, Ltd. (1995).
11. A. JONSSON and R. REC, "Nodal Imbedded Calculation for the Retrieval of Local Power Peaking from Coarse Mesh Reactor Analysis," *Proc. Intl. Topical Meeting on Advance in Mathematical Methods for the Solution of Nuclear Engineering Problems*, Munich, W. Germany, April, Vol. II, p. 23 (1981).
12. "HELIOS Methods," Scanpower (1994).
13. P. J. DAVIS, *Interpolation and Approximation*, Dover Publications, Inc., New York (1975).
14. P. LANCATER and K. SALKAUSKAS, *Curve and Surface Fitting*, Academic Press, San Diego, California (1988).
15. K. L. DERSTINE, "DIF3D: A Code to Solve One-, Two-, and Three-Dimensional Finite-Difference Diffusion Theory Problems," ANL-82-64, Argonne National Laboratory (April 1984).

Table 1. Cardinal Functions of Reconstruction Method I

$$F^{av}(x,y)=\frac{9}{4}-9x^2-9y^2+36x^2y^2$$

$$F_1^s(x,y)=-\frac{3}{8}+\frac{3}{2}x+\frac{9}{2}x^2+\frac{3}{2}y^2-6xy^2-18x^2y^2$$

$$F_1^c(x,y)=\frac{1}{16}-\frac{1}{4}x-\frac{3}{4}x^2-\frac{1}{4}y+xy+3x^2y-\frac{3}{4}y^2+3xy^2+9x^2y^2$$

$$F_i^a(x,y)=F_1^a(x_i,y_i),\qquad a=s,c\quad (i=2,3,4)$$

$$\begin{pmatrix}x_i\\y_i\end{pmatrix}=\begin{bmatrix}\cos\theta_i & \sin\theta_i\\ -\sin\theta_i & \cos\theta_i\end{bmatrix}\begin{pmatrix}x\\y\end{pmatrix},\qquad \theta_i=\frac{i-1}{2}\pi$$

Table 2. Cardinal Functions of Reconstruction Method II

$$F^{av}(x,y)=3-18x^2-18y^2+36x^2y^2+30x^4+30y^4$$

$$F_1^s(x,y)=-\frac{9}{16}+2x+9x^2+\frac{3}{2}y^2-6xy^2-18x^2y^2-2x^3-15x^4$$

$$F_1^c(x,y)=\frac{1}{16}-\frac{1}{4}x-\frac{3}{4}x^2-\frac{1}{4}y+xy+3x^2y-\frac{3}{4}y^2+3xy^2+9x^2y^2$$

$$F_1^J(x,y)=-\frac{1}{32}+\frac{1}{4}x+\frac{3}{4}x^2-x^3-\frac{5}{2}x^4$$

$$F_i^a(x,y)=F_1^a(x_i,y_i),\qquad a=s,c,J\quad (i=2,3,4)$$

$$\begin{pmatrix}x_i\\y_i\end{pmatrix}=\begin{bmatrix}\cos\theta_i & \sin\theta_i\\ -\sin\theta_i & \cos\theta_i\end{bmatrix}\begin{pmatrix}x\\y\end{pmatrix},\qquad \theta_i=\frac{i-1}{2}\pi$$

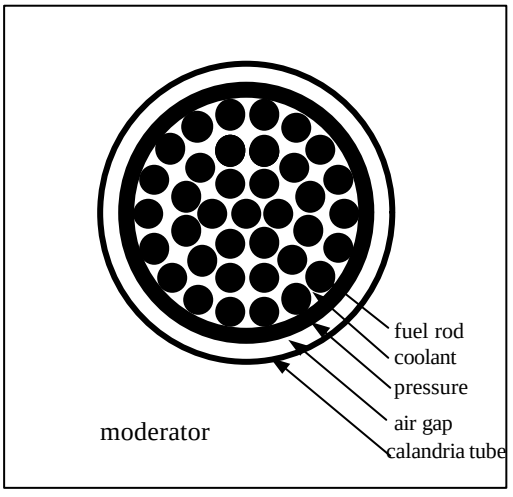

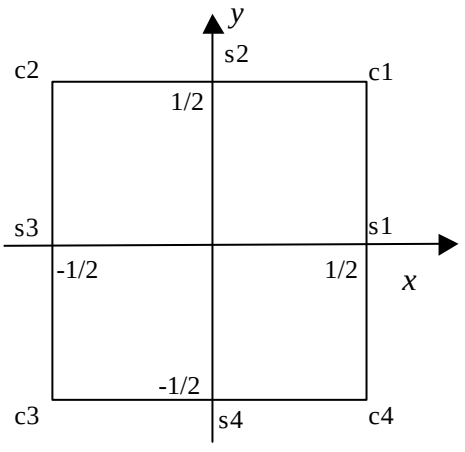

7500	**7500**	**3200**
-3.145	-3.081	-2.742
-1.744	-1.772	-0.847
-1.890	-1.940	-1.000
3200	**0**	**7500**
0.833	-2.174	-3.081
1.889	2.132	-1.787
1.697	1.758	-1.950
3200	**3200**	**7500**
0.540	0.802	-3.173
2.364	1.852	-1.752
2.111	1.664	-1.893

Burnup(Mwd/t)
Fast flux
Thermal flux
Pin power

(a) 3-by-3 Fuel Bundle Problem

5400	**431**	**2156**	**226**	**3868**	**5400**
0.556	0.741	1.370	-1.318	-2.138	-3.434
1.822	3.467	2.804	2.065	-0.708	-1.878
1.696	3.184	2.560	1.773	-0.823	-2.069
1294	**3200**	**5183**	**3200**	**6469**	**1294**
0.306	0.859	-0.679	-1.041	-3.096	-3.052
2.755	2.329	1.297	0.816	-1.612	-0.839
2.509	2.186	1.148	0.660	-1.830	-0.999
4090	**6041**	**863**	**5828**	**2365**	**3868**
-1.465	-1.416	-1.417	-1.909	-2.561	-3.277
0.437	0.175	1.428	-0.614	-0.659	-1.500
0.317	-0.265	1.141	-0.803	-0.813	-1.662
6675	**1725**	**3645**	**1725**	**5183**	**6675**
-2.969	-1.785	-1.285	-2.061	-3.263	-4.526
-1.371	0.896	0.557	0.623	-1.619	-2.973
-1.571	0.586	0.429	0.339	-1.753	-3.183
2574	**4530**	**6469**	**4530**	**1078**	**2574**
-2.153	-1.760	-2.492	-1.570	-2.480	-2.729
-0.328	-0.362	-0.984	-0.377	0.396	-0.917
-0.475	-0.487	-1.212	-0.487	-0.186	-1.057
5400	**431**	**2156**	**226**	**3868**	**5400**
-2.362	-1.928	-0.745	-1.994	-1.836	-3.522
-1.037	1.191	1.144	1.267	-0.505	-1.944
-1.234	0.884	0.883	0.997	-0.608	-2.114

(b) 6-by-6 Fuel Bundle Problem

Fig. 3. Maximum Reconstruction Errors (%) in Pin-wise Flux and Power.

7500	**7500**	**3200**
0.336	0.557	0.433
0.682	0.417	0.131
0.612	0.371	0.112
3200	**0**	**7500**
0.696	-0.116	0.561
-0.540	-0.427	-0.391
-0.514	-0.379	0.352
3200	**3200**	**7500**
-0.285	0.687	0.332
0.172	-0.533	0.663
0.119	-0.503	0.591

Burnup(Mwd/t)
Fast flux
Thermal flux
Pin power

(a) 3-by-3 Fuel Bundle Problem

5400	**431**	**2156**	**226**	**3868**	**5400**
0.404	-0.480	0.469	-0.739	0.527	0.342
0.227	-0.143	-0.195	-0.197	-0.113	0.185
0.223	-0.128	-0.205	-0.193	-0.121	0.172
1294	**3200**	**5183**	**3200**	**6469**	**1294**
-0.133	0.581	0.265	0.682	0.118	0.202
0.171	-0.135	0.276	-0.203	0.175	-0.165
-0.150	-0.139	0.239	-0.189	0.134	-0.169
4090	**6041**	**863**	**5828**	**2365**	**3868**
0.468	0.272	-0.191	0.350	0.449	0.335
0.274	0.154	0.145	0.135	0.087	0.232
-0.262	0.140	0.115	0.129	0.094	-0.226
6675	**1725**	**3645**	**1725**	**5183**	**6675**
0.276	0.382	0.456	0.270	0.467	0.193
0.222	-0.153	-0.064	0.163	0.127	0.223
0.186	-0.153	-0.062	0.138	0.117	0.183
2574	**4530**	**6469**	**4530**	**1078**	**2574**
0.386	0.648	0.121	0.742	-0.256	0.493
-0.207	-0.081	0.177	-0.074	-0.205	-0.207
-0.212	0.089	0.139	0.066	-0.227	-0.209
5400	**431**	**2156**	**226**	**3868**	**5400**
0.385	-0.463	0.492	-0.725	0.541	0.261
0.219	-0.168	-0.272	-0.132	0.118	0.273
0.215	-0.172	-0.278	0.118	0.128	0.253

(b) 6-by-6 Fuel Bundle Problem

Fig. 4. Maximum Interpolation Errors (%) in Pin-wise Flux and Power.

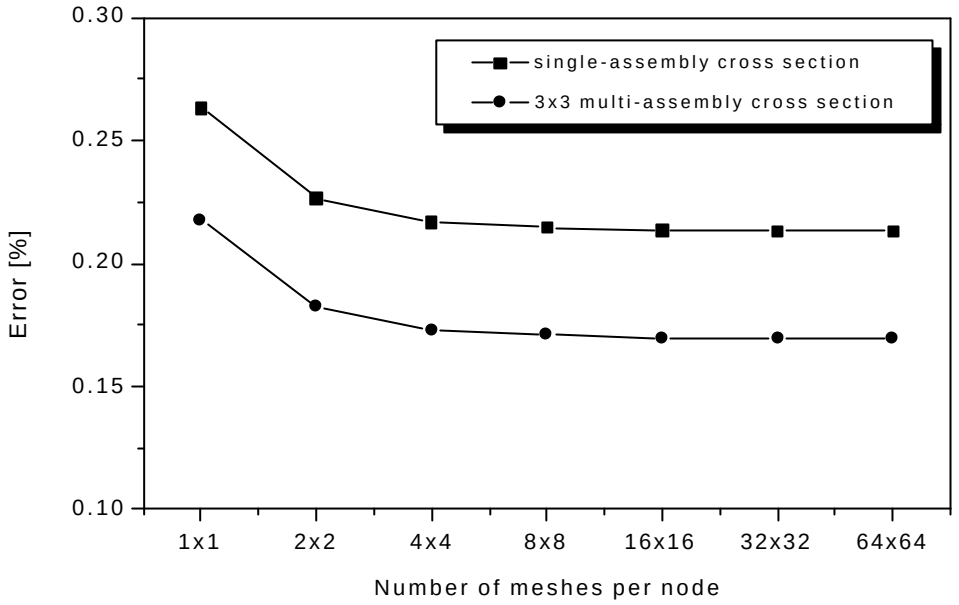

Fig. 5. Multiplication Factor Error vs. Mesh Size of 3-by-3 Problem.